Hindawi Publishing Corporation
Journal of Nanomaterials
Volume 2015, Article ID 694234, 7 pages
http://dx.doi.org/10.1155/2015/694234

Research Article

Enhancement of Two-Dimensional Electron-Gas Properties by Zn Polar ZnMgO/MgO/ZnO Structure Grown by Radical-Source Laser Molecular Beam Epitaxy

Li Meng,[1,2,3] Jingwen Zhang,[1,2,3] Qun Li,[1,2,3] and Xun Hou[1]

[1]*Key Laboratory of Photonics Technology for Information, Xi'an Jiaotong University, Xi'an, Shaanxi 710049, China*
[2]*Key Laboratory for Physical Electronics and Devices under Ministry of Education, Xi'an Jiaotong University, Xi'an, Shaanxi 710049, China*
[3]*Joint Laboratory of Functional Materials and Devices for Informatics, Xi'an Jiaotong University and Institute of Semiconductors, CAS, Xi'an, Shaanxi 710049, China*

Correspondence should be addressed to Jingwen Zhang; jwzhang@mail.xjtu.edu.cn

Received 19 January 2015; Accepted 9 March 2015

Academic Editor: Meiyong Liao

A Zn polar ZnMgO/MgO/ZnO structure with low Mg composition $Zn_{1-x}Mg_xO$ layer ($x = 0.05$) grown on a-plane (11–20) sapphire by radical-source laser molecular beam epitaxy was reported. The insertion of a thin (1 nm) MgO layer between ZnMgO and ZnO layers in the ZnMgO/ZnO 2DEG structures results in an increase of 2DEG sheet density and affects electron mobility slightly. The carrier concentration reached a value as high as 1.1×10^{13} cm^{-2}, which was confirmed by C-V measurements. A high Hall mobility of 3090 cm^2/Vs at 10 K and 332 cm^2/Vs at RT was observed from $Zn_{0.95}Mg_{0.05}O$/MgO/ZnO heterostructure. The choice of the thickness of MgO was discussed. The dependence of carrier sheet density of 2DEG on ZnMgO layer thickness was calculated in theory and the theoretical prediction and experimental results agreed well.

1. Introduction

ZnO and its heterostructures, which have several advantages including a high saturation velocity [1], a large conduction band offset for ZnMgO/ZnO heterostructures [2], and the possibility to form a high-density two-dimensional electron-gas (2DEG) [3], have great potential for high-frequency and high-power device applications. So far, the formation of 2DEG at Zn polar $Zn_{1-x}Mg_xO$/ZnO interface has been observed by a few groups using molecular beam epitaxy (MBE) [4–8], pulse laser deposition (PLD) techniques [9], metal-organic vapor phase epitaxy (MOVPE) [10], and RF sputtering [11]. However, in low Mg composition $Zn_{1-x}Mg_xO$/ZnO heterostructures ($x < 0.1$) high electron mobility can be observed but with very low 2DEG sheet density ($n < 10^{12}$ cm^{-2}) [12], and in high Mg composition $Zn_{1-x}Mg_xO$/ZnO heterostructures ($x > 0.1$), 2DEG sheet density reached a considerable value (10^{12} ~10^{13} cm^{-2}) but electron mobility is still deeply affected by alloy disorder scattering, especially at low temperatures. In addition the obtained mobility in previous papers was lower than 250 cm^2/Vs at RT [13]. It has been reported that modified AlGaN/AlN/GaN structures, which employ a thin AlN interfacial layer between AlGaN and GaN layers, show higher 2DEG properties than those of conventional AlGaN/GaN structures. This is reported to be a result of the reduction of alloy disorder scattering due to the suppression of carrier penetration from the GaN channel into the AlGaN layer [14–17]. However, the inserting of MgO into ZnMgO/ZnO structure has never been reported. In this work, we report a Zn polar ZnMgO/MgO/ZnO structure to enhance two-dimensional electron-gas properties and discuss the dependence of carrier sheet density of 2DEG on ZnMgO layer thickness which was calculated in theory and the theoretical prediction and experimental results agreed well.

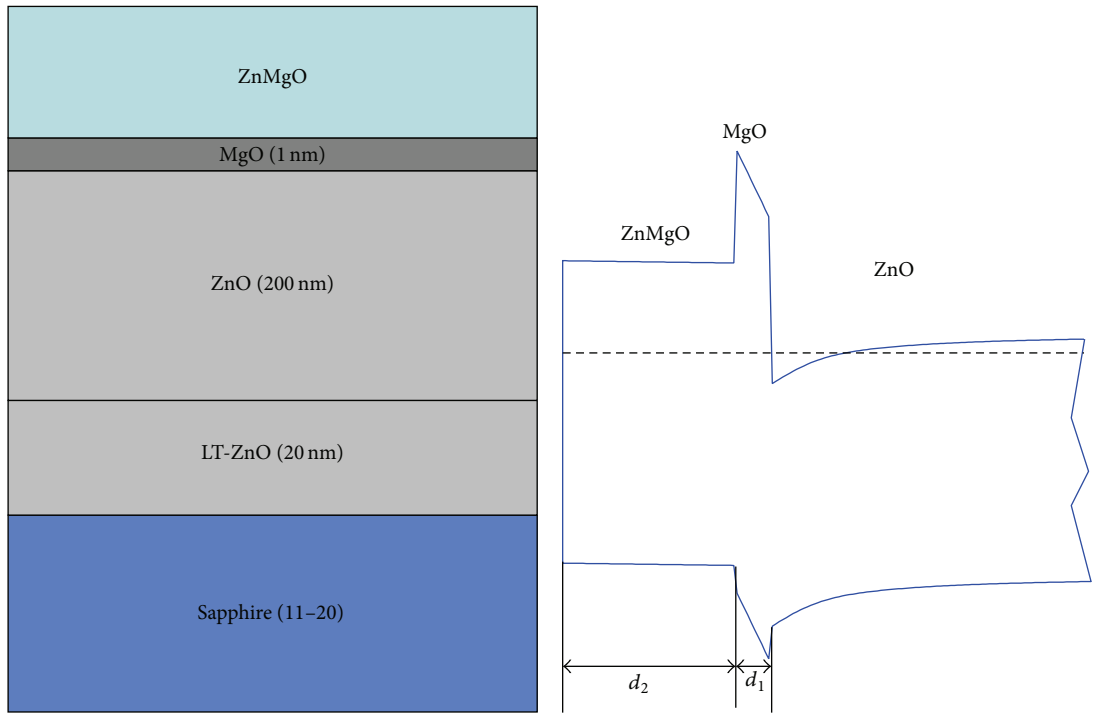

Figure 1: Layer structure (a) and band diagram (b) for a Zn polar ZnMgO/MgO/ZnO heterostructure. The growth direction is <0001> for Zn polarity.

2. Materials and Methods

Zn polar ZnMgO/ZnO and ZnMgO/MgO/ZnO heterostructures were all grown on sapphire (11–20) substrates by radical-source laser molecular beam epitaxy (RS-LMBE) system (Shenyang Scientific Instrument Co., Ltd., Chinese Academy of Sciences (SKY)). The 5 N purity of ZnO target was vaporized by KrF excimer laser (Lambda Physik, COMPex 102, 248 nm, 1–20 Hz, 100 mJ). At first, the substrates were treated by nitrogen plasma, which was ionized by radio-frequency (rf) plasma source (Oxford Applied Research, HD-25) at 700°C for 1 h to obtain nitrogen polarity surface and control the growth of single-domain Zn polar ZnO film [18]. The growth was conducted in an oxygen pressure of 10^{-3} Pa. A 20 nm thick low temperature- (LT-) ZnO buffer layer was deposited at 250°C. Secondly, a 200 nm undoped ZnO layer was deposited at 700°C. Finally, an undoped ZnMgO layer was grown at 400°C. For ZnMgO/MgO/ZnO heterostructures (Figure 1(a)), the MgO was deposited before the growth of ZnMgO layer under same condition with ZnMgO layer. The crystalline qualities of the thin films were studied by Philips X'Pert PW3040 high resolution X-ray diffraction (XRD) system using Cu Kα (λ = 0.15406 nm). The growth evolution of MgO layer and the choice of its thickness were investigated by the streaky patterns of the reflection high-energy electron diffraction (RHEED). The Mg composition (x) was determined from the reflectance measurement of the exciton band gap energy of $Zn_{1-x}Mg_xO$ using the equation $E_g(x) = E_g(0) + 2.145x$ [19]. The crystal polarity was determined based on differences in etching-rate between Zn polar and O-polar samples. Chemical wet etching was carried out using 0.01 M hydrochloric acid solution at room temperature, for etching-rate measurements [20]. The capacitance-voltage (C-V) measurement was performed by using mercury contacts. The electrical properties were examined by Lake Shore 7707A Hall mobility system in a van der Pauw configuration with a magnetic-field of 1000 G.

3. Results and Discussion

3.1. The Thickness of the MgO Insert Layer. To optimize the MgO thickness and make sure that the MgO has grown as wurtzite structure, the growth evolution of MgO layer was investigated by RHEED pattern, shown as in Figure 2. Initially, the MgO layer grew 2-dimensionally on c-ZnO as the thickness was 0.5 and 1 nm in Figures 2(a) and 2(b). Then the growth mode of MgO layer changes from 2-dimensional to 3-dimensional. When the MgO thickness was 1.5 nm, the RHEED spots appeared (Figure 2(c)), which suggests that the crystal structure of the MgO layer changes with increasing layer thickness. Therefore, in this paper, a 1 nm MgO layer was chosen.

3.2. Structural Property. Figure 3 shows the XRD spectra for the grown ZnMgO/MgO/ZnO structure on sapphire substrate. Because of the low concentration of Mg in the ZnMgO layer, the ZnO (0002) peak and ZnMgO (0002) are overlapped. The crystal quality of the $Zn_{0.95}Mg_{0.05}O$/MgO/ZnO

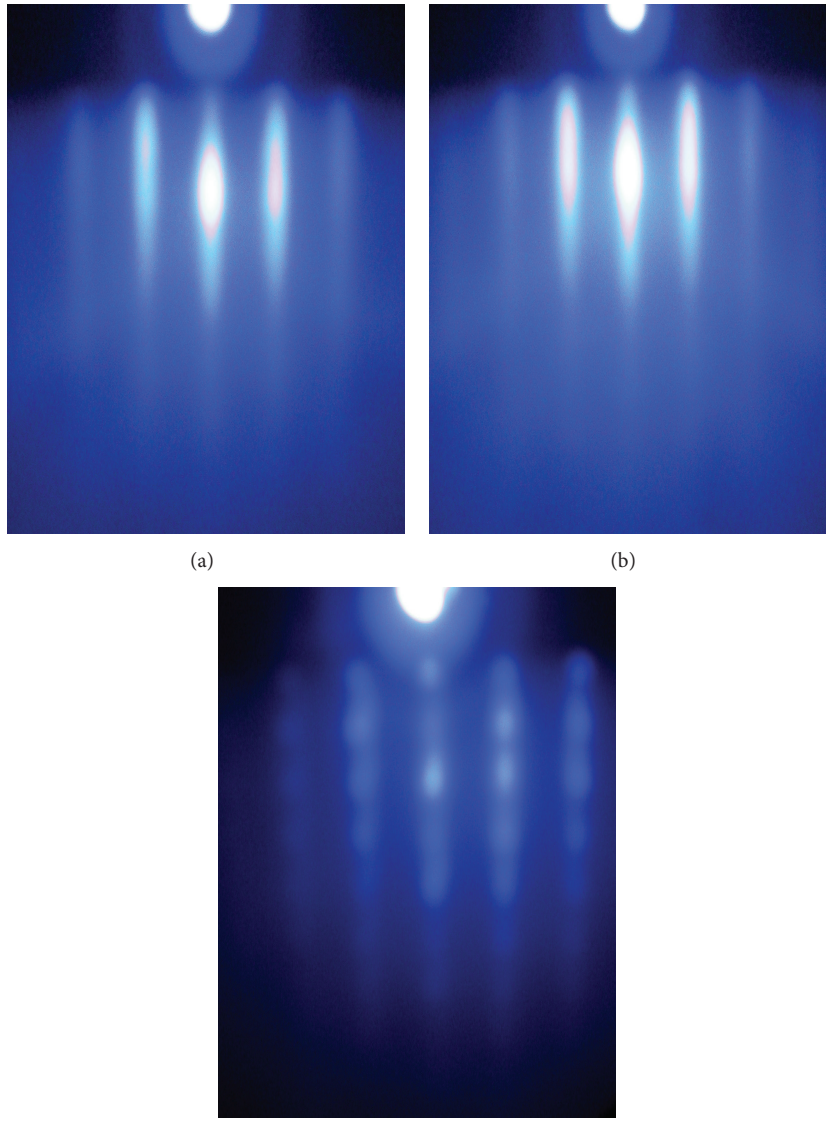

Figure 2: The evolution of RHEED pattern during growth of the MgO layer. The direction of MgO is <11–20>. (a) The thickness of the MgO buffer layer is 0.5 nm; (b) thickness of MgO = 1 nm; and (c) thickness of MgO = 1.5 nm.

structure was characterized by a cross-sectional TEM image (JEM-2100F). A typical image recorded near the ZnMgO/MgO/ZnO interface is shown in the inset of Figure 3. The interface could not be detected in the TEM micrograph clearly, which suggests that the structure has a high degree of crystalline quality. The MgO has no phase transition from wurtzite structure to rock salt structure. High electron mobility will benefit from the enhanced structure and crystal quality. It also can be observed that the MgO interfacial layer is grown with a thickness of approximately 1 nm, which corresponds to the designed thickness.

3.3. Electrical Property. Figure 4 displays carrier density derived from capacitance as a function of distance from the top surface for the $Zn_{0.95}Mg_{0.05}O$/ZnO and $Zn_{0.95}Mg_{0.05}O$/MgO/ZnO structures, and both of the thicknesses of $Zn_{0.95}Mg_{0.05}O$ layers are 100 nm. It shows that high concentration 2DEG was confined at the interface. Formation of 2DEG at the interface was demonstrated by the features. Comparing with $Zn_{0.95}Mg_{0.05}O$/ZnO structure, a sharp 2DEG peak is shown around interface in $Zn_{0.95}Mg_{0.05}O$/MgO/ZnO structure without penetration into the $Zn_{1-x}Mg_xO$ layer, which behaves similarly with previous report about AlGaN/AlN/GaN [14]. From these results, it can be concluded that the thin MgO interfacial layer effectively suppresses carrier penetration into the ZnMgO layer and enhances the confinement of 2DEG in ZnO channel. In addition, a sheet carrier concentration of 1.1×10^{13} cm^{-2} was observed in the $Zn_{0.95}Mg_{0.05}O$/MgO/ZnO structure with 20 nm thick $Zn_{0.95}Mg_{0.05}O$ layer confirmed by

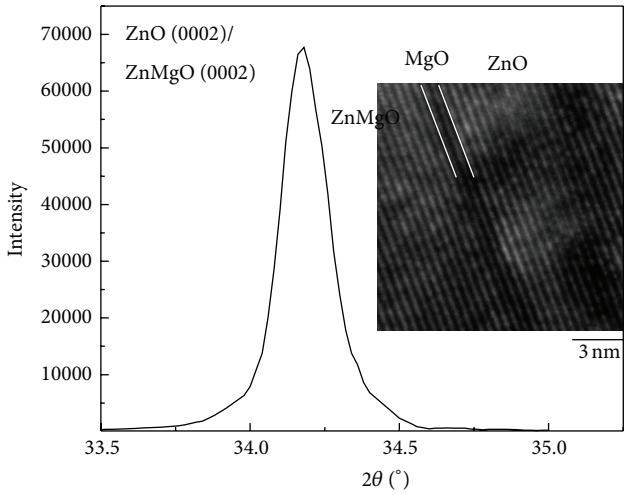

Figure 3: The XRD spectra for the grown ZnMgO/MgO/ZnO structure; the inset is the cross-sectional TEM image of a ZnMgO/MgO/ZnO film.

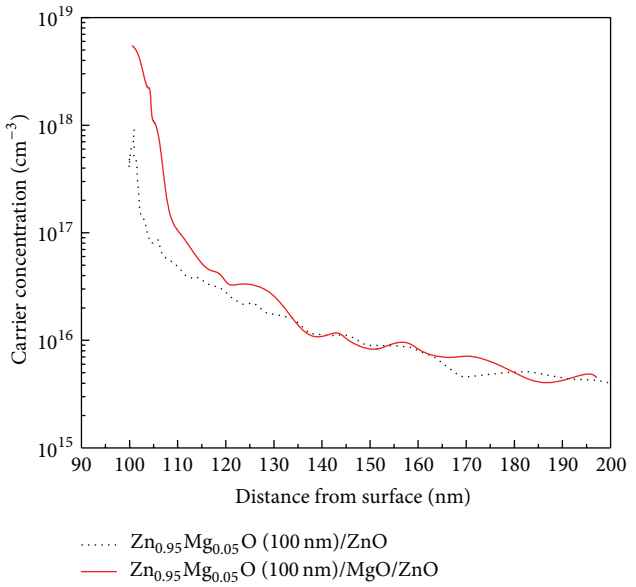

Figure 4: *C-V* depth profiling of the 2DEG and net donor concentration in the $Zn_{0.95}Mg_{0.05}O$/ZnO and $Zn_{0.95}Mg_{0.05}O$/MgO/ZnO structures.

C-V measurement. 2DEG of $Zn_{0.95}Mg_{0.05}O$/ZnO structure with 20 nm thick $Zn_{0.95}Mg_{0.05}O$ layer was not observed by *C-V*. Owing to the low Mg content and thickness of ZnMgO barrier layer, the conduction band offset was small and the providing of electron was not enough to format 2DEG.

Table 1 shows the typical values of Hall mobility (μ) and 2DEG density (n) measured at 300 K and 10 K for ZnMgO/ZnO structures with or without MgO interfacial layers. From Table 1, it is clearly seen that the Hall mobility was increased by the insertion of MgO interfacial layers. In particular, the $Zn_{0.95}Mg_{0.05}O$ (20 nm)/MgO/ZnO heterostructure showed very high Hall mobility of 332 cm^2/Vs at RT and 3090 cm^2/Vs at 10 K. Figure 5 shows the results of temperature-dependent Hall measurements. The electron mobility of $Zn_{0.95}Mg_{0.05}O$ (100 nm)/ZnO and $Zn_{0.95}Mg_{0.05}O$ (100 nm and 20 nm)/MgO/ZnO structures increases with decreasing temperature, as shown in Figure 5(a). This trend is nearly identical to that reported for AlGaAs/GaAs [21–23], AlGaN/GaN [24, 25], and ZnMgO/ZnO heterostructure [5, 13], which is consistent with the existence of a 2DEG at the heterointerface. Compared with reported values for both Zn polar and O-polar ZnMg(Mn)O/ZnO heterostructures, the high mobility is obvious [11, 13, 26, 27]. The mobility of $Zn_{0.95}Mg_{0.05}O$ (20 nm)/ZnO structure changed similarly to a single ZnO thin film as the temperature was changing, which indicates no 2DEG was formatted because of thin barrier layer. By the insertion of MgO layer, a 2DEG was observed. The results agree well with the results of *C-V* measurement. The high electron mobility of the ZnMgO/MgO/ZnO heterostructure was mainly attributed to the reduction of alloy disorder scattering. In Figure 5(b), the sheet carrier concentration of $Zn_{0.95}Mg_{0.05}O$ (100 nm)/ZnO and $Zn_{0.95}Mg_{0.05}O$ (100 nm and 20 nm)/MgO/ZnO structures changes little with increasing temperatures, indicating the good confinement of channel electrons. The insert of a thin (1 nm) MgO layer between ZnMgO and ZnO enhanced the sheet carrier concentration almost one order of magnitude. It also confirms the thin MgO enhanced the confinement effectively.

Table 1: Typical Hall mobility (μ) and 2DEG density (n) measured at 300 K and 10 K for ZnMgO/ZnO structures with or without MgO interfacial layers.

Structure	ZnMgO thickness (nm)	n ($\times 10^{12}$ cm^{-2})		μ (cm^2/Vs)	
		300 K	10 K	300 K	10 K
ZnMgO/MgO/ZnO	20	25	22	332	3090
ZnMgO/ZnO	20	1.5	0.2	137	130
ZnMgO/MgO/ZnO	100	2.2	1.9	321	2480
ZnMgO/ZnO	100	0.2	0.4	215	2360

3.4. The Calculation and Experimental Results of the Dependence of Carrier Sheet Density of 2DEG on ZnMgO Layer Thickness. It is noted that the presence of strong polarization-induced fields in both MgO and ZnMgO cap layers leads to a very interesting dependence of the 2DEG sheet density in ZnMgO/MgO/ZnO structures on ZnMgO cap thickness. The density of 2DEG decreases with increasing ZnMgO thickness. To discuss the behavior of 2DEG density changing with the thickness of ZnMgO layer in ZnMgO/MgO/ZnO structures, simple electrostatic analysis of the $Zn_{1-x}Mg_xO$/MgO/ZnO heterostructures yields the following expression for the 2DEG sheet density [11, 15, 28–30]:

$$n_S = \frac{1}{1 + d_1/d_2}\left[\frac{+\sigma}{e} - \frac{\varepsilon_0 \varepsilon}{d_2}\left(e\phi_b + E_F - \Delta E_C\right)\right], \quad (1)$$

where the effect of $Zn_{1-x}Mg_xO$ cap was approximately equal to a ZnO cap layer because of the low Mg composition and where d_1 (1 nm here) and d_2 are the thicknesses of the MgO and top $Zn_{1-x}Mg_xO$ layer barrier layers, correspondingly,

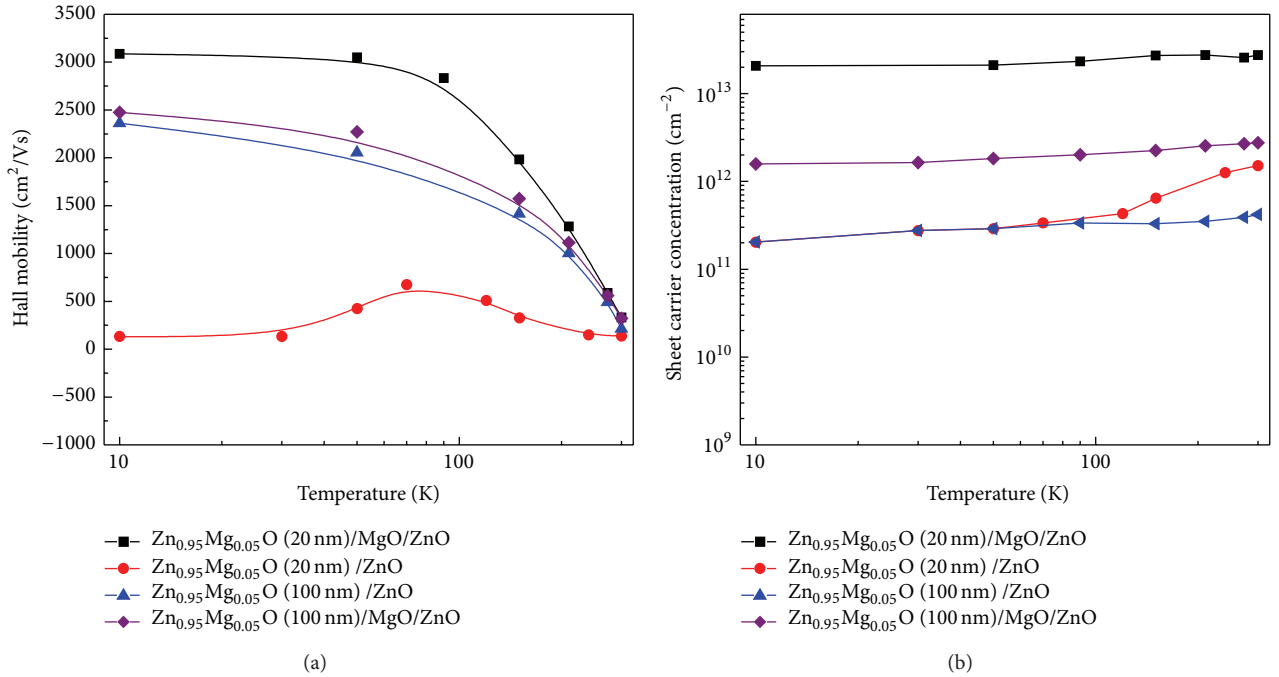

FIGURE 5: Temperature-dependent Hall measurements for Zn polar $Zn_{0.95}Mg_{0.05}O$/ZnO and $Zn_{0.95}Mg_{0.05}O$/MgO/ZnO structures, mobility (a) and carrier concentration (b).

as shown in Figure 1(b); the surface potential $e\phi_b$ is assumed to be pinned at surface with a level of 0.8 eV below ZnO conduction band edge. The conduction band offset ΔE_C is equal to $0.9 \times [E_g(\text{MgO}) - E_g(\text{ZnO})]$ [31]. We approximate the Fermi level E_F by the infinite triangular quantum well [23], which can be expressed as

$$E_F = \left[\frac{9\pi\hbar e^2}{\left(8\varepsilon_0\sqrt{8m^*}\right)}\frac{n_S}{\varepsilon}\right]^{2/3} + \frac{\pi\hbar^2}{m^* n_S}, \quad (2)$$

where the dielectric constant ε is given as $(8.75 + 1.08 * 1)$ for the very thin wurtzite MgO [10]. The effective mass is taken to be $m^* \approx 0.26m_e$. σ is the polarization-induced charge density determined by the vector sum of the spontaneous polarization (P_{SP}) and the strain-induced piezoelectric polarization (P_{PE}) while there is no external field. We assume that the thin MgO layer is fully strained on ZnO and polarization constants vary linearly with x composition. Thus, the dependence of total polarizations-induced charges in MgO layer can be expressed as $\sigma = 0.029x\,(\text{C/m}^2)$ $(x = 1)$ [12]. Taking the tunneling of electrons from MgO/ZnO channel to $Zn_{1-x}Mg_xO$ layer into account, we modified σ by a coefficient v, and then it can be expressed as

$$\sigma = 0.029v\left(\text{C/m}^2\right), \quad (v = 0 \sim 1). \quad (3)$$

For $v = 0.1$, the calculated 2DEG density and experimental results were shown in Figure 6. The solid line is the calculated plot extracted from (1). The sheet carrier concentration decreases rapidly as the thickness of ZnMgO layer increases. The 2DEG density of the $Zn_{0.95}Mg_{0.05}O$/MgO/ZnO

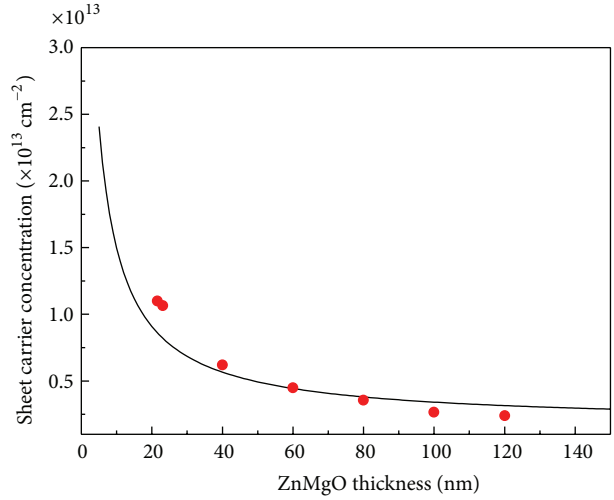

FIGURE 6: The dependence of sheet carrier concentration as a function of ZnMgO layer thickness.

structure with the layer thickness of 20 nm is 1.1×10^{13} cm^{-2}, and it becomes 2.4×10^{12} cm^{-2} when the thickness is 120 nm. The theoretical prediction and experimental results agreed well below 80 nm, which confirmed the ZnMgO layers in ZnMgO/MgO/ZnO structure, to a certain extent, behaved similar to a ZnO cap layer. After the thickness became larger than 80, the 2DEG density became lower than the calculated line. That is because the stress of the ZnMgO strain layer increases as the thickness increases, which results in the

deterioration of crystal quality. There might be other reasons which need to be studied in the future.

We note that there is somewhat a discrepancy in the sheet carrier concentration values obtained by C-V and Hall measurement. Since the data observed from Hall measurement includes the contribution of bulk carrier, the value was higher than the true value.

4. Conclusion

In summary, formation of a 2DEG was confirmed for Zn polar ZnMgO/ZnO heterostructures with low Mg composition ($x = 0.05$). The enhancement of 2DEG concentration and mobility were realized in $Zn_{1-x}Mg_xO$/MgO/ZnO with low Mg composition by inserting of a thin (1 nm) MgO obviously. The sample shows a high Hall mobility of 3090 cm^2/Vs at 10 K and 332 cm^2/Vs at RT. The carrier concentration reached a value as high as 1.1×10^{13} cm^{-2}. However, the study for higher Mg content $Zn_{1-x}Mg_xO$/MgO/ZnO structures will be done in the future. The results demonstrate a well defined heterostructure and the possibility for fabrication of ZnMgO/MgO/ZnO HEMT devices.

Conflict of Interests

The authors declare that there is no conflict of interests regarding the publication of this paper.

Acknowledgments

This work was supported by Project 863 of Xi'an Jiaotong University (2013AA03A101) and National Natural Science Foundation of China (no. 60876042 and no. 61176018).

References

[1] J. D. Albrecht, P. P. Ruden, S. Limpijumnong, W. R. L. Lambrecht, and K. F. Brennan, "High field electron transport properties of bulk ZnO," *Journal of Applied Physics*, vol. 86, no. 12, pp. 6864–6867, 1999.

[2] A. Ohtomo, M. Kawasaki, T. Koida et al., "$Mg_xZn_{1-x}O$ as a II-VI widegap semiconductor alloy," *Applied Physics Letters*, vol. 72, no. 19, pp. 2466–2468, 1998.

[3] A. Ohtomo, M. Kawasaki, I. Ohkubo, H. Koinuma, T. Yasuda, and Y. Segawa, "Structure and optical properties of ZnO/$Mg_{0.2}Zn_{0.8}O$ superlattices," *Applied Physics Letters*, vol. 75, no. 7, pp. 980–982, 1999.

[4] H. Tampo, H. Shibata, K. Maejima et al., "Polarization-induced two-dimensional electron gases in ZnMgO/ZnO heterostructures," *Applied Physics Letters*, vol. 93, no. 20, Article ID 202104, 3 pages, 2008.

[5] A. Tsukazaki, A. Ohtomo, M. Kawasaki et al., "Spin susceptibility and effective mass of two-dimensional electrons in $Mg_xZn_{1-x}O$/ZnO heterostructures," *Physical Review B*, vol. 78, no. 23, Article ID 233308, 2008.

[6] S. Sasa, M. Ozaki, K. Koike, M. Yano, and M. Inoue, "High-performance ZnO/ZnMgO field-effect transistors using a hetero-metal-insulator-semiconductor structure," *Applied Physics Letters*, vol. 89, no. 5, Article ID 053502, 2006.

[7] K. Koike, D. Takagi, M. Kawasaki et al., "Ion-sensitive characteristics of an electrolyte-solution-gate ZnO/ZnMgO heterojunction field-effect transistor as a biosensing transducer," *Japanese Journal of Applied Physics*, vol. 46, no. 36-40, pp. L865–L867, 2007.

[8] K. Koike, D. Takagi, M. Hashimoto et al., "Characteristics of enzyme-based ZnO/$Zn_{0.7}Mg_{0.3}O$ heterojunction field-effect transistor as glucose sensor," *Japanese Journal of Applied Physics*, vol. 48, no. 4, Article ID 04C081, 2009.

[9] M. Nakano, A. Tsukazaki, A. Ohtomo et al., "Electronic-field control of two-dimensional electrons in polymer-gated-oxide semiconductor heterostructures," *Advanced Materials*, vol. 22, no. 8, pp. 876–879, 2010.

[10] J. D. Ye, S. Pannirselvam, S. T. Lim et al., "Two-dimensional electron gas in Zn-polar ZnMgO/ZnO heterostructure grown by metal-organic vapor phase epitaxy," *Applied Physics Letters*, vol. 97, no. 11, Article ID 111908, 2010.

[11] H.-A. Chin, I.-C. Cheng, C.-K. Li et al., "Electrical properties of modulation-doped rf-sputtered polycrystalline MgZnO/ZnO heterostructures," *Journal of Physics D: Applied Physics*, vol. 44, no. 45, Article ID 455101, 4 pages, 2011.

[12] A. Tsukazaki, H. Yuji, S. Akasaka et al., "High electron mobility exceeding $10^4 Cm^2 v^{-1}$ s^{-1} in $Mg_xZn_{1-x}O$/ZnO single heterostructures grown by molecular beam epitaxy," *Applied Physics Express*, vol. 1, no. 5, Article ID 055004, 2008.

[13] H. Tampo, H. Shibata, K. Matsubara et al., "Two-dimensional electron gas in Zn polar ZnMgO/ZnO heterostructures grown by radical source molecular beam epitaxy," *Applied Physics Letters*, vol. 89, no. 13, Article ID 132113, 3 pages, 2006.

[14] M. Miyoshi, T. Egawa, H. Ishikawa et al., "Nanostructural characterization and two-dimensional electron-gas properties in high-mobility AlGaN/AlN/GaN heterostructures grown on epitaxial AlN/sapphire templates," *Journal of Applied Physics*, vol. 98, no. 6, Article ID 063713, 5 pages, 2005.

[15] I. P. Smorchkova, L. Chen, T. Mates et al., "AlN/GaN and (Al,Ga)N/AlN/GaN two-dimensional electron gas structures grown by plasma-assisted molecular-beam epitaxy," *Journal of Applied Physics*, vol. 90, no. 10, pp. 5196–5201, 2001.

[16] L. Shen, S. Heikman, B. Moran et al., "AlGaN/AlN/GaN high-power microwave HEMT," *IEEE Electron Device Letters*, vol. 22, no. 10, pp. 457–459, 2001.

[17] L. Hsu and W. Walukiewicz, "Effect of polarization fields on transport properties in AlGaN/GaN heterostructures," *Journal of Applied Physics*, vol. 89, no. 3, pp. 1783–1789, 2001.

[18] Z. X. Mei, Y. Wang, X. L. Du et al., "Controlled growth of O-polar ZnO epitaxial film by oxygen radical preconditioning of sapphire substrate," *Journal of Applied Physics*, vol. 96, no. 12, pp. 7108–7111, 2004.

[19] H. Tampo, H. Shibata, K. Maejima et al., "Strong excitonic transition of $Zn_{1-x}Mg_xO$ alloy," *Applied Physics Letters*, vol. 91, no. 26, Article ID 261907, 3 pages, 2007.

[20] J. S. Park, S. K. Hong, T. Minegishi et al., "Polarity control of ZnO films on (0001) Al_2O_3 by Cr-compound intermediate layers," *Applied Physics Letters*, vol. 90, no. 20, Article ID 201907, 3 pages, 2007.

[21] R. Dingle, H. L. Störmer, A. C. Gossard, and W. Wiegmann, "Electron mobilities in modulation-doped semiconductor heterojunction superlattices," *Applied Physics Letters*, vol. 33, no. 7, pp. 665–667, 1978.

[22] S. Hiyamizu, T. Mimura, T. Fujii, and K. Nanb, "High mobility of two-dimensional electrons at the GaAs/n-AlGaAs heterojunction interface," *Applied Physics Letters*, vol. 37, no. 9, pp. 805–807, 1980.

[23] S. hiyamizu and T. Mimura, "High mobility electrons in selectively doped GaAs/n-AlGaAs heterostructures grown by MBE and their application to high-speed devices," *Journal of Crystal Growth*, vol. 56, no. 2, pp. 455–463, 1982.

[24] M. A. Khan, J. M. Van Hove, J. N. Kuznia, and D. T. Olson, "High electron mobility GaN/$Al_xGa_{1-x}N$ heterostructures grown by low-pressure metalorganic chemical vapor deposition," *Applied Physics Letters*, vol. 58, no. 21, pp. 2408–2410, 1991.

[25] M. A. Khan, J. N. Kuznia, J. M. Van Hove, N. Pan, and J. Carter, "Observation of a two-dimensional electron gas in low pressure metalorganic chemical vapor deposited GaN-$Al_xGa_{1-x}N$ heterojunctions," *Applied Physics Letters*, vol. 60, no. 24, pp. 3027–3029, 1992.

[26] T. Edahiro, N. Fujimura, and T. Ito, "Formation of two-dimensional electron gas and the magnetotransport behavior of ZnMnO/ZnO heterostructure," *Journal of Applied Physics*, vol. 93, no. 10, pp. 7673–7675, 2003.

[27] K. Koike, K. Hama, I. Nakashima et al., "Piezoelectric carrier confinement by lattice mismatch at ZnO/$Zn_{0.6}Mg_{0.4}O$ heterointerface," *Japanese Journal of Applied Physics*, vol. 43, no. 10, pp. L1372–L1375, 2004.

[28] O. Ambacher, B. Foutz, J. Smart et al., "Two dimensional electron gases induced by spontaneous and piezoelectric polarization in undoped and doped AlGaN/GaN heterostructures," *Journal of Applied Physics*, vol. 87, no. 1, pp. 334–344, 2000.

[29] I. P. Smorchkova, C. R. Elsass, J. P. Ibbetson et al., "Polarization-induced charge and electron mobility in AlGaN/GaN heterostructures grown by plasma-assisted molecular-beam epitaxy," *Journal of Applied Physics*, vol. 86, no. 8, pp. 4520–4526, 1999.

[30] E. T. Yu, G. J. Sullivan, P. M. Asbeck, C. D. Wang, D. Qiao, and S. S. Lau, "Measurement of piezoelectrically induced charge in GaN/AlGaN heterostructure field-effect transistors," *Applied Physics Letters*, vol. 71, no. 19, pp. 2794–2796, 1997.

[31] M. Yano, *Zinc Oxide, Bulk, Thin Films and Nanostructures*, C. Jagadish and S. J. Pearton, Eds., Elsevier, Amsterdam, The Netherlands, 2006.